Swelling behaviour of poly(methylmethacrylate) thick resist layers in deep X-ray lithography

C. Khan Malek[a,b*] and S. Das[b]

[a]Laboratoire de Spectroscopie Atomique et Ionique, CNRS-UMR8624, Université Paris-Sud, Batiment 350, 91405 Orsay CEDEX, France, and [b]Center for Advanced Microstructures and Devices (CAMD), Louisiana State University, 6980 Jefferson Highway, Baton Rouge, LA 70806, USA. E-mail: chantal.khan-malek@cnrs-dir.fr

The understanding and optimization of lithographic conditions are particularly important for irradiation of thick resist layers in deep X-ray lithography. The causes and consequences of radiation-induced formation and accumulation of gaseous species inside the poly(methylmethacrylate) (PMMA) resist matrix are discussed. Thick PMMA layers were exposed to high-energy photons from a bending-magnet beamline at the Center for Advanced Microstructures and Devices (CAMD). The focus of this work was to explore the swelling behaviour of PMMA resist of thickness between 50 μm and 1.6 mm. The influence of various exposure parameters, such as photon energy, filtering conditions, electron current in the storage ring, scan length and scan speed, exposure atmosphere *etc.*, on the swelling of the resist are discussed. The effect of pre-exposure annealing of the PMMA sheets and of temperature variation during irradiation was also investigated. Exposure with optimized X-ray spectral distribution, incident power density, absorbed dose and rate of energy deposition inside the resist allowed swelling of the resist to be minimized during exposure.

Keywords: poly(methylmethacrylate); deep X-ray lithography; LIGA; thick resist; swelling.

1. Motivation and aim of this study

The LIGA process (Becker *et al.*, 1986) and variants are used for the production of high-aspect-ratio and high-precision microcomponents and microsystems by synchrotron X-ray printing followed by electro\-forcelb]forming and eventually molding. Poly(methylmethacrylate) (PMMA) is the X-ray-sensitive resist generally used for the first step of the process, the deep X-ray lithography step. In X-ray lithography the absorber pattern on the mask is transferred into the resist by shadow casting of a mask placed in proximity to the resist layer utilizing synchrotron radiation. The penetration depth of the high-energy X-rays is taken advantage of for producing very tall pseudo-three-dimensional microstructures. The patterned resist serves as a template for subsequent electroforming, and is then removed at the end of the process when electroformed molds or parts have been formed.

PMMA is a polymer that is easily degraded by ionizing radiation. It has been widely used as a standard resist in a variety of lithographic applications, mainly with X-ray, electron or ion beams (Moreau, 1988; Moore & Choi, 1991). The lithographic properties of a polymer resist depend on the physico–chemical modifications inside the polymeric material produced under radiation. The radiation chemistry and structural changes of PMMA under UV, soft X-ray, hard X-ray and γ-rays have been studied by various authors (Moreau, 1988; Moore & Choi, 1991; Hiraoka, 1977; Lehockey *et al.*, 1988; Garrett *et al.*, 1991; Ichikawa & Yoshida, 1994; Yates & Shinozaki, 1993; Tinone & Tanaka, 1995; Okudaira *et al.*, 1998) but few have worked on thick PMMA films under conditions similar to those for the LIGA process (Schmalz *et al.*, 1996; Wollersheim *et al.*, 1995; Wollersheim & Hormes, 1996; Waali *et al.*, 1998). The photochemical reaction pathways depend on many factors, in particular the energy of the radiation. There seems to be a consensus that the main degradation process in the energy range corresponding to X-rays and γ-radiation occurs by main-chain scission at low radiation doses (Moreau, 1988; Lehockey *et al.*, 1988) following a pathway different from that of heat-induced decomposition (Moreau, 1988). For all practical purposes in our studies, PMMA is a positive-tone resist, which degrades with a reduction of molecular mass of the polymer, resulting in an increase of dissolution rate of the exposed regions in a 'developer' solution to form three-dimensional microstructures. This degradation is also accompanied by the formation of smaller molecular products and gaseous fragments, resulting in material loss and generation of microporosity in the resist bulk. Although these studies are beyond the scope of this report, much work still needs to be done to characterize the physico–chemical processes occurring upon irradiation of thick polymer resist as well as the diffusion mechanisms of the by-products within the polymer matrix.

In conventional X-ray lithography of very-high-resolution advanced integrated circuits, resist layer thicknesses of 1 μm or less are used. In deep X-ray lithography for microelectromechanical systems (MEMS), resist thicknesses of hundreds of micrometers to millimeters (and more) are used, which generates different issues. Lithography of thick PMMA resist layers requires long exposure times for a sufficient dose to be absorbed in each volume element, from the surface to the bottom of the resist layer, to ensure complete development of the irradiated structures. If a threshold dose or a dose rate is exceeded, an excessive gas release may accumulate within the resist bulk and cause resist expansion and 'swelling' of the resist or even foaming of the exposed region. (Fig. 1). This swelling may cause

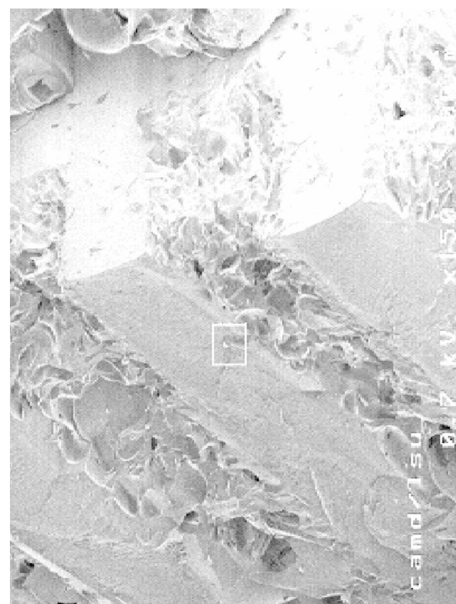

Figure 1
Swelling of PMMA under exposure. Maximum measured swelling $\simeq$ 670 μm of 1 mm-thick PMMA CQ grade, not annealed, and irradiated using 90 × 90 μm wire-mesh mask, average current I = 193 mA, ring energy = 1.3 GeV, scan length = 1.25 cm (0.5″), scan velocity = 6.25 mm s^{-1} (0.25″ s^{-1}). Dose at the resist bottom = 3 kJ cm^{-3}.

 © 2003 International Union of Crystallography • Printed in Great Britain – all rights reserved

various problems during the lithographic step and have consequences for the following steps of the LIGA process:

(i) Deformations and cracks in the polymers can result in possible loss of geometrical accuracy of the pattern and structural fracture of the material.

(ii) Built-up stress in the polymer matrix (Moldovan, 1999) can lead to changes in the material properties, particularly mechanical properties, as well as debonding at the resist–substrate interface ('popping' of the resist layer).

(iii) Limitation of the minimum proximity gap between the PMMA resist layer and the X-ray mask during the printing process is necessary to avoid damage to the mask. This precaution is particularly critical if a fragile membrane is being used as in many exposures performed with medium-energy X-rays (under 15 keV). A large gap setting may deteriorate the quality of pattern transfer, particularly for small features, owing to diffraction and beam divergence.

(iv) The use of conformal masks fabricated directly on the resist layer leads to a greater sensitivity to irradiation and development conditions, especially for multiple pattern transfer in very thick resist. They require minimizing the amount of swelling which would irreversibly damage the conformal mask and distort pattern features.

The exposure requirements need to be optimized for each particular system 'source/scanner/mask/resist' (Henry *et al.*, 1998; De Carlo *et al.*, 1998).

In this work, the lithographic conditions for pattern transfer with minimum resist swelling into thick PMMA commercial layers, in particular clinical-grade high-molecular-weight ICI PMMA, were investigated by deep X-ray lithography at CAMD. Parameters influencing resist swelling were studied for PMMA thicknesses varying from 50 µm to 1.6 mm in order to optimize exposure conditions. The swelling behaviour was analyzed as a function of exposure conditions such as total absorbed dose, uniformity of dose distribution and rate of dose deposition, as well as intrinsic resist properties such as variations in chemical structure/composition and resist treatment. Other effects, such as the influence of temperature on swelling during irradiation, were also investigated as we were exploring exposure strategies to reduce swelling.

2. Experimental

Most of the PMMA samples were solvent-bonded with the monomer, MMA, on silicon substrate and fly cut (Chaudhuri *et al.*, 1997) to thicknesses from 50 to 1500 µm; some others were used as free-standing sheets.

The exposures were performed on a bending magnet of the CAMD storage ring operating with an electron energy of 1.3 or 1.5 GeV, corresponding to a photon critical energy of 1.7 and 2.6 keV (0.74 and 0.48 nm), respectively. The 7B-XRLM3 beamline for deep X-ray lithography had a 125 µm-thick Be window, which functioned as a high-pass filter, transmitting a broadband spectrum for photon energies above 1.5 keV, typically 2–10 keV. A variety of exposure parameters were used: different electron energy and beam current in the ring, filtering, scan length and velocity, helium pressure, and masks. All the experiments were performed with either the same mask with 2 µm-thick silicon membrane and 6 µm gold absorber or a mesh mask with 90 µm × 90 µm-wide openings. The mask/wafer assembly was mounted on a simple lead screw-driven scanner stage powered by a stepper motor. The scan range was limited (7 cm) and the scan speed was relatively low (0.25–12.7 mm s^{-1}). In particular, the scan speed and acceleration time were fixed, which implies that our exposure system did not compensate for variations of stored current in the ring, and hence changes in X-ray fluxes and instantaneous dose rate incident on the resist. PMMA of thicknesses up to 300 µm were exposed with the ring operating at 1.3 GeV, and thickness above 300 µm at 1.5 GeV.

The lithographic sensitivity of the resist was expressed in equivalent incident radiation doses as the current stored in the ring multiplied by the time taken to obtain a specified change in the normalized film thickness after development. The doses were calculated using *CXrL Toolset* (CXrL Toolset, 1966). The intensity–time product (mA min) corresponding to exposures with a bottom volume dose of 3 kJ cm^{-3} was administered to the PMMA resist unless otherwise specified. The incident power density was calculated for the average current during exposure (I_{avg}). The exposure time was given by the ratio of the equivalent dose by the average current.

Local swelling on various spots of the resist resulted from exposure to radiation through printing various transparent areas of the mask carrying the same repeated pattern. The height differences were measured using a surface profilometer (Alphastep 500 from Tencor Instruments) within the first 20–30 min after exposure, unless otherwise specified. The values displayed below in the tables and figures are average values. Despite good resolution of the profilometer (0.1, 2.5 and 15.5 nm nominal accuracy for scans of maximum vertical amplitude variation of 13 µm, 300 µm and 2 mm, respectively), topographical roughness of the radiation-induced swollen portions of the resist precluded accurate measurement of the swelling amplitude below 50 nm and in the worst cases, where the resist was foamed, below 1 µm.

To study the variation in swelling while modifying the resist temperature during irradiation, a brass back-plate with an in-built zigzag copper tubing was built to hold the wafer/mask substrate. The temperature of the glycol fluid passing through the tubing was regulated between 269 and 318 K using a thermostat (with heater/cooler) from outside the chamber. The whole set-up including the wafer with PMMA resist, the mask and backplate was installed in the chamber and scanned in the beam during the experiment.

3. Results

3.1. Swelling as a function of PMMA material and thermal pre-exposure treatment

Acrylic sheets of an unknown source purchased from AIN Plastics (regular 1.6 mm-thick or custom-ordered 230 µm-thick material) or from Goodfellow (ICI, Perspex, 1 mm-thick, CQ grade) were exposed as-received under similar conditions (Table 1). The response of the PMMA sheets, though globally similar under X-ray radiation and development, led to different radiation-induced swelling amplitudes, the lower being observed using PMMA from AIN Plastics. PMMA may differ by several factors: molecular weight and distribution, crystallinity, tacticity, impurity content, thermal treatment as received *etc*. Our standard PMMA source for this work, ICI, was cell-cast linear syndiotactic-rich PMMA with an approximate molecular weight of 5 000 000 and a 5% MMA monomer content (Henry *et al.*, 1999). Thermal treatment of ICI PMMA before exposure resulted in controlled swelling as exemplified in Table 1 and Fig. 2. The radiation-induced swelling amplitude on annealed ICI samples was recorded here from immediately after exposure to a period of two months after exposure. Annealed PMMA at 333 K for 24 h showed neither any significant reduction in swelling during exposure nor any significant variation in swelling post-exposure. Warping was observed when annealing at 373 K for 1 h. The optimum annealing procedure for these ICI 1 mm-thick PMMA samples in terms of temperature and time length was at 353 K for 1 h (the ramping up and down being performed at 3 K min^{-1}). Annealing at 353 K reduced the swelling

Table 1
Swelling of acrylic sheet with resist source and pre-exposure thermal treatment.

Exposure conditions: ring electron energy = 1.3 GeV, 125 μm-thick Be window, 25 torr He atmosphere, dose at bottom of resist = 3 kJ cm^{-3}, no filter, 2.0 μm Si membrane, scan length = 2.5 cm, scan velocity = 6.25 mm s^{-1}. Pre-exposure annealing conditions of PMMA sheet: annealing temperature for 1 h, nitrogen atmosphere, temperature ramped up and down at 3 and 1 K min^{-1}, respectively.

PMMA thickness and source	Pre-exposure annealing	Equivalent dose (mA min)	I_{avg} (mA)	Exposure time (min)	Swelling after exposure (μm)	Swelling after 5 d (μm)	Swelling after 14 d (μm)
230 μm AIN	Not annealed	4220	139	30	63	–	–
250 μm ICI (CQ)	Not annealed	4670	180	26	310	–	–
250 μm ICI (CQ)	Not annealed	4670	102	26	114	114	114
250 μm ICI (CQ)	333 K, 24 h	4670	133	26	98	98	112
250 μm ICI (CQ)	333 K, 1 h	4670	180	26	85	87	87
250 μm ICI (CQ)	353 K, 1 h	4670	126	26	27	91	106
250 μm ICI (CQ)	373 K, 1 h	4670	137	26	31	105	118

during exposure while not causing warping of the PMMA sheets during annealing. However, it did not suppress time-induced swelling of the PMMA after exposure. For PMMA annealed both at 353 K and 373 K a significant increase in swelling was found after five days, and eventually the swelling amplitude became comparable to the swelling of PMMA that had not been annealed previously.

3.2. Swelling as a function of PMMA thickness and filtering conditions

The production of volatile fragments is much more important in thicker resists, causing more swelling. Photons of various energies, corresponding to various penetration depths, are incident on the resist. The resist acts as a filter and the deposited energy decreases as a function of depth within the resist thickness. Absorption of low-energy photons occurs at the resist surface, resulting in higher doses at the surface, leading to more swelling. In particular, it can cause damage before the bottom of the resist receives a sufficient minimum dose for formation of a three-dimensional profile after development.

Filtering is designed to remove the low-energy part of the spectrum. It also modifies the spectral distribution of the spectrum incident on the resist and shifts it towards harder X-ray photons, as shown in Fig. 3. This corresponds to a larger penetration depth of the X-rays and a more uniform dose deposition through the resist thickness, translating into a smaller ratio of top-to-bottom dose. Filtering therefore reduced swelling, as observed in Table 2. Under our exposure conditions, an additional aluminium thickness of approximately 3 μm was required for each 50 μm of PMMA when exposed with a 2 μm silicon mask membrane with a maximum current of 150 mA at energy 1.3 GeV. The results, presented in Table 2 and Fig. 4, demonstrate that there was an optimal filtration for each resist thickness.

For 300 μm-thick resist exposed at high current, above 200 mA, a 9 μm-thick Al filter was required for minimizing the PMMA swelling, whereas with a lower current, 123 mA, the exposures could be performed using less filtering (6 μm Al). The relevant parameter for this series of tests for exposure with minimum swelling was the incident power density on the resist, which was itself

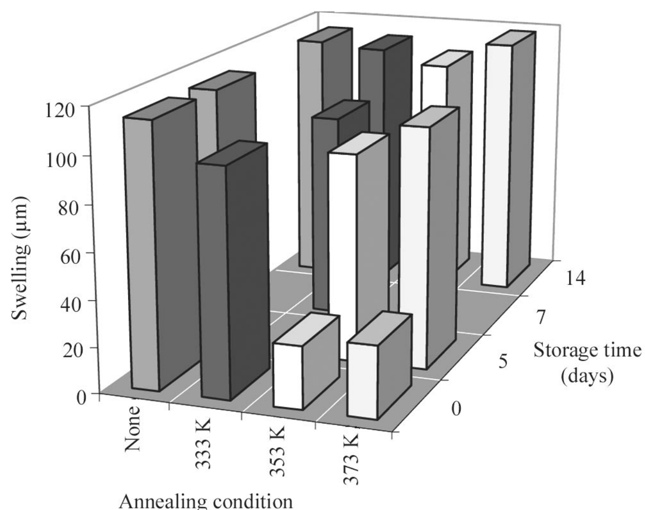

Figure 2
Variation in swelling due to pre-exposure annealing and storage time after exposure. Same conditions as in Table 1.

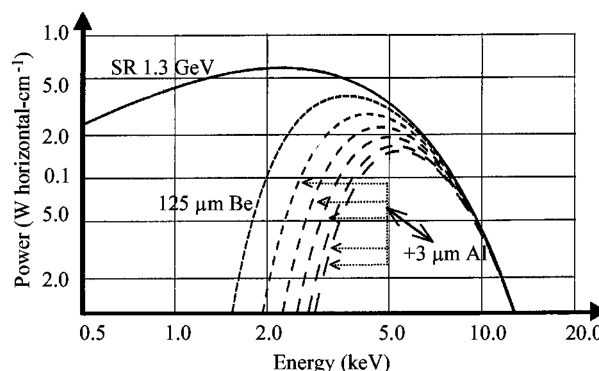

Figure 3
Calculated incident spectral distribution on the mask with various filters. Synchrotron radiation power spectrum from a bending-magnet source and transmitted spectra through various filters on the 7B-XRLM3 beamline. Parameters in the calculation using *CXrL Toolset* (CXrL Toolset, 1966): storage ring operated at 1.3 GeV; distance to X-ray source = 10 m; no optical element; 125 μm Be window; radiative power normalized to 100 mA ring current. The five spectra at the outmost right correspond to additional filtering with an incremental 3 μm Al filter added for each spectrum from left to right.

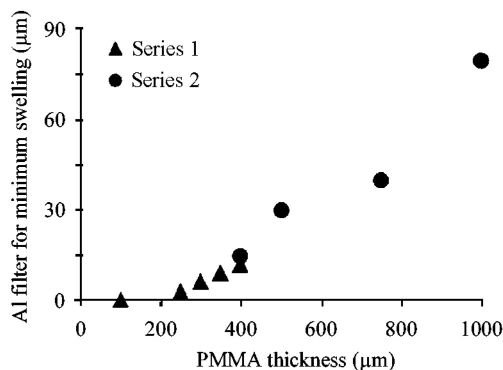

Figure 4
Filtering thickness (Al filter) necessary for minimum swelling as a function of PMMA thickness. Series 1: exposure with a 2 μm-thick Si mask membrane and CAMD ring operating at 1.3 GeV. Series 2: exposure with free-standing mesh mask and CAMD ring operating at 1.5 GeV. The accuracy of the filter thickness is within 3 μm as this was our increment for filtering addition. For the accuracy of swelling measurements, see §2.

Table 2
Swelling results with variation in resist thickness and filtering conditions.

Exposure conditions: XRLM3 beamline; 125 µm Be window; 25 torr He; ICI (CQ) PMMA, not annealed; bottom dose 3 kJ cm^{-3}, scan length 2.5 cm, scan velocity 6.25 mm s^{-1}.

PMMA thickness (µm)	Ring energy (GeV)	Mask	Al filter thickness (µm)	I_{avg} (mA)	Exposure time (min)	Incident power density (W horiz-cm^{-1})	Top/bottom power ratio	Maximum swelling (µm)
100	1.3	2 µm Si	None	121	15	34.5	4.0	0
250	1.3	2 µm Si	None	180	26	51.0	10.4	310
250	1.3	2 µm Si	3	186	31	25.1	6.1	1
300	1.3	2 µm Si	None	48	122	13.5	13.0	40
300	1.3	2 µm Si	None	148	40	41.6	13.0	268
300	1.3	2 µm Si	6	123	69	10.2	5.5	0
300	1.3	2 µm Si	6	249	34	20.6	5.5	40
300	1.3	2 µm Si	9	211	47	12.0	4.4	4
350	1.3	2 µm Si	6	177	57	14.6	6.5	96
350	1.3	2 µm Si	9	122	95	6.9	5.2	0
400	1.3	2 µm Si	3	205	49	27.2	10.6	219
400	1.3	2 µm Si	12	116	132	4.8	5.0	0
100	1.3	Mesh	None	123	11	59.5	5.1	14
300	1.3	Mesh	None	127	40	60.7	19.1	183
300	1.5	Mesh	None	117	15	103.9	12.0	214
400	1.5	Mesh	None	123	20	107.8	16.7	376
400	1.5	Mesh	6	74	43	18.9	6.4	163
400	1.5	Mesh	12	71	56	9.3	4.1	64
400	1.5	Mesh	15	67	66	6.9	3.6	0
500	1.5	Mesh	30	79	103	3.4	2.8	0
750	1.5	Mesh	26	68	154	3.5	4.3	261
750	1.5	Mesh	40	70	198	2.0	3.2	0
1000	1.5	Mesh	60	112	218	1.7	3.0	170
1000	1.5	Mesh	70	104	270	1.3	2.7	170
1000	1.5	Mesh	80	94	340	0.9	2.5	8
1600	1.5	Mesh	70	93	457	1.2	4.2	374

a function of the current in the ring. The incident power density tolerable for non-swelling conditions on the resist depended on the thickness of the resist and the current in the ring, as well as the filtering conditions. For example, for exposures at 1.3 GeV with a 2 µm silicon mask membrane, minimum swelling was obtained for 100 µm-thick PMMA receiving an incident power of 35 W horizontal-cm^{-1} whereas, for 300 µm-thick PMMA, 10–12 W horizontal-cm^{-1} was the threshold above which the resist swelled. For 100 µm-thick resist, this was achieved using a non-filtered incident beam, whereas for thicker 300 µm PMMA, a 6 or 9 µm-thick Al filter was needed depending on the current intensity, 123 or 211 mA, respectively. Swelling did not depend only on the top-to-bottom ratio, as is exemplified in Table 2. For example, two different beam currents, 123 and 249 mA, led to different swelling amplitudes, under the limit of detection of the equipment used and 40 µm, respectively, for 300 µm-thick PMMA samples exposed with the same top/bottom dose ratio of 5.5 and the same filtering conditions. Also, very thick resist layers of thicknesses 1000 and 1600 µm, both exposed with a top-to-bottom ratio smaller than 5, swelled by 170 and 374 µm, respectively. The thicker the resist, the lower the threshold in terms of incident power density to cause swelling. As the filters attenuated the intensity of the beam by absorbing the lower-energy part at the expense of the overall power on the resist, exposure times became longer (Fig. 5). For example, two exposure conditions for a 300 µm-thick PMMA resist led to a 40 µm-thick swelling, one with a high current, 249 mA, and filtration of 6 µm aluminium, the other corresponding to an extreme low case of 48 mA current without filter. This increase in current by a factor of five reduced the exposure time per inch scan length by a factor of approximately 3.6 (34 min *versus* 122 min). The amount of swelling that was tolerable depended on the projected application as well as the processes following the lithography. We commonly worked with a swelling up to one-third of the value of the resist thickness.

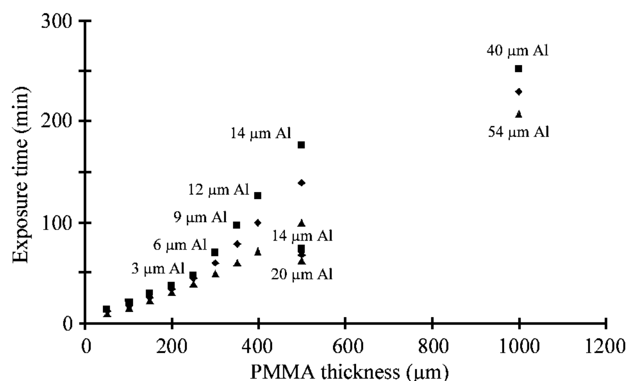

Figure 5
Variation of exposure time as a function of PMMA thickness. A 2 µm-thick silicon membrane was used for exposure of the non-annealed PMMA samples on beamline XRLM3, scan length 2.25 cm. The shapes of the points indicate the energy E and average electron current (Avg. I) of operation of the CAMD storage ring as well as filtering conditions. Squares: E = 1.3 GeV, Avg. I = 150 mA, best filter thickness for minimum swelling indicated on the graph; the two first square points corresponding to less than 150 µm-thick resist did not need filtering. Diamonds: E = 1.3 GeV, Avg. I = 150 mA, no filter. Triangles: E = 1.5 GeV, Avg. I = 90 mA, no filter.

3.3. Swelling as a function of bottom dose

A higher bottom dose, corresponding to a larger incident equivalent dose, caused increased swelling of the resist (Table 3). This result was consistent with a larger production of gases within the resist.

3.4. Swelling as a function of critical energy of radiation

The operation of the ring at higher electron energy (E) corresponded to both (i) a shift in the spectral distribution of the synchrotron radiation spectrum to higher energy (critical energy E_c proportional to E^3) and (ii) an increase in output power [P (W $mrad^{-1}$) = E^3 (GeV) × B (T) × I (A), where B and I are the magnetic field current and the stored current in the ring, respectively].

When changing the operation of the ring from 1.3 to 1.5 GeV electron energy with the same stored current in the ring, the critical photon energy shifted from 1.7 to 2.6 keV and the output power of the ring increased by a factor of 1.2, from 1.4 to 2.4 W $mrad^{-1}$, causing more swelling (Table 4). This effect will be enhanced by using the superconducting magnets of the wiggler instead of the conventional bending magnets of the storage ring: a critical energy of 11.2 keV at 7.5 T maximum magnetic field of the wiggler (1.5 GeV electron energy for the ring) giving an output power (10.7 W $mrad^{-1}$) that is increased by a factor of four compared with operation at 1.5 GeV with the same stored current in the ring. The increase of power incident on the resist leads to a higher dose deposition rate, and therefore to a higher production rate of gaseous by-products and more swelling of the resist.

Table 3
Swelling results with variation in dose.

Same conditions as Table 2 except for the bottom doses.

PMMA thickness (μm)	Ring energy (GeV)	Mask	Al filter thickness (μm)	Bottom dose (kJ cm^{-3})	I_{avg} (mA)	Exposure time (min)	Incident power density (W horiz-cm^{-1})	Top/bottom power ratio	Maximum swelling (μm)
250	1.3	2 μm Si	None	1	164	10	46.4	10.4	0
250	1.3	2 μm Si	None	3	180	26	51.0	10.4	310
250	1.3	2 μm Si	None	5	184	42	52.0	10.4	340
1000	1.5	Mesh	50	1.8	96	132	2.0	3.5	0
1000	1.5	Mesh	50	3	88	239	1.8	3.5	80

Table 4
Swelling results with variation in ring energy.

Same conditions as Table 2. Mask: mesh; filter: none.

PMMA thickness (μm)	Ring energy (GeV)	I_{avg} (mA)	Exposure time (min)	Incident power density (W horiz-cm^{-1})	Top/bottom power ratio	Maximum swelling (μm)
300	1.3	127	40	60.66	19.1	183
300	1.5	117	15	103.9	12.0	214

Table 5
Swelling results with variation of stored current in the ring.

Same conditions as Table 2. Mask: 2 μm Si; filter: none.

PMMA thickness (μm)	Al filter (μm)	I_{avg} (mA)	Exposure time (min)	Incident power density (W horiz-cm^{-1})	Top/bottom power ratio	Maximum swelling (μm)
250		102	46	28.9	10.4	114
250		180	26	51.0	10.4	310
300		48	122	13.5	6.1	40
300		148	40	41.6	13.0	268
300	6	123	69	10.2	5.5	0
300	6	249	34	20.6	5.5	40

3.5. Swelling as a function of electron current in the ring

Higher current in the ring also resulted in higher incident power on the resist, leading to more swelling (Table 5).

3.6. Influence of the exposure system and environment on swelling

3.6.1. Scan length and velocity of exposure. A decrease in scan velocity, which corresponded to an increase of dose deposition rate, gave rise to more swelling (the effect was more visible with no filter where the swelling amplitude was larger). On the other hand, an increase in scan length at fixed speed corresponded to an increase in swelling. Increased scan length allowed for more time between each scan at a particular location on the resist, which allowed the produced gases to diffuse causing the top resist layer to swell. As might be expected, this effect was less pronounced with filtering. The results are compiled in Table 6.

3.6.2. He pressure in chamber. The exposures were performed in a chamber with a static He gas pressure, which provided an inert atmosphere for both the beryllium window and the resist during irradiation. The He atmosphere also permitted heat transfer to the environment by convection, in particular from the mask and to a certain extent from the wafer. The influence of the variation of the He pressure in the chamber on the swelling is presented in Table 7. No significant difference in swelling was observed between 1 torr He pressure and the normally used 25 torr He pressure. If the pressure was further decreased (0.6–0.7 torr), more swelling was observed. The lower pressure probably helped the gaseous by-products to diffuse out of the PMMA more easily. Moreover, the cooling efficiency was reduced with lower He pressure, which might have increased the swelling, as will be discussed in §3.6.3. On the other extreme, exposure at higher pressure from 200 torr to atmospheric pressure outside the sample resulted in a significant reduction in swelling by counteracting the radiation-induced built-up pressure within the PMMA.

3.6.3. Measurement of the temperature rise during exposure. Experiments were performed at 1.3 and 1.5 GeV in helium atmosphere (25 torr) while scanning the sample in the beam under various exposure conditions. The temperature was recorded during exposure with a commercial precision fine-wire thermocouple (J-type thermocouple iron/Constantan from Omega). The tip of the thermocouple was maintained in contact with the surface of a 1.6 mm-thick resist pad. When no filter was used, the resist was completely decomposed and became a foam. The maximum temperature obtained when the sample was scanned in and out of the beam with no mask and an electron stored current of 145–150 mA was approximately 363 and 423 K, respectively, representing a temperature differential of 60 K. A higher helium pressure or the presence of a 3 μm Al filter decreased the temperature rise, 343–378 K and 363–378 K, respectively, and reduced the magnitude of the temperature differential to 35 and 15 K, respectively. When a free-standing mesh metallic mask was used to expose the resist, the temperature and temperature differential dropped further: 343–353 K and 10 K. An additional 3 μm-thick Al filter caused a larger decrease: 335–341 K. The filtering power of 460 μm-thick PMMA was also investigated and resulted in no difference of temperature between the areas in and out of the X-ray beam: 345 K/347 K. Despite the fact that the current in the ring was decreasing as the experiment was progressing, the trend observed here was very clear.

More swelling could be expected with a higher temperature conducive to a faster diffusion rate of gases in the resist matrix. However, at temperatures above the glass temperature the resist integrity was destroyed. One could expect that even if the resist still worked at higher temperature the accuracy of the pattern transfer would be affected by the mismatch of thermal expansion coefficients of the mask, substrate and resist materials.

3.6.4. Backplate temperature. The wafers used for this series of experiments were coated with 300 μm-thick PMMA. The swelling resulting from exposure to X-rays through the transparent areas of a large mesh mask was measured at three different locations on the wafer within the first 20–30 min after the exposure. The experiments were conducted at four different temperatures between 269 and 318 K. Consistent results in the swelling variation with respect to the backplate temperature were obtained. They are summarized in Fig. 6. We can see that the swelling amplitude increased with increasing temperature and that the swelling amplitude was higher at 1.5 GeV than at 1.3 GeV, as expected from previous results.

4. Discussion

For thin PMMA films, dose deposition is relatively simple, and diffusion of the radiation-induced gases takes place rapidly so no accumulation of gases inside the resist occurs. Moreover, the short exposure times limit the thermal damage to the resist even at high incident power. With the thick and very thick PMMA layers used in

Table 6
Swelling results with variation in scan length and scan velocity.

Same conditions as Table 2 except for scan length and velocity. Mask: 2 µm Si.

PMMA thickness (µm)	Ring energy (GeV)	Filter	Scan length (cm)	Scan velocity (mm s^{-1})	I_{avg} (mA)	Exposure time (min)	Incident power density (W horiz-cm^{-1})	Top/bottom power ratio	Maximum swelling (µm)
250	1.3	None	1.5	1.25	150	19	42.5	10.4	151
250	1.3	None	1.5	12.5	155	18	43.9	10.4	125
250	1.3	3 µm Al	2.5	12.5	186	31	25.1	6.1	1
250	1.3	3 µm Al	2.5	6.25	204	28	27.5	6.1	2
250	1.3	3 µm Al	4	6.25	199	46	26.8	6.1	42
250	1.3	3 µm Al	6.25	6.25	201	72	27.1	6.1	47

Table 7
Swelling results with variation in He pressure.

Same conditions as Table 2 except for He pressure. Mask: 2 µm Si.

PMMA thickness (µm)	He pressure (torr)	Filter	I_{avg} (mA)	Exposure time (min)	Incident power density (W horiz-cm^{-1})	Top/bottom power ratio	Maximum swelling (µm)
250	0.73	3 µm Al	173	33	23.35	6.1	131
250	25	3 µm Al	204	28	27.5	6.1	2
250	25	None	180	26	51.0	10.4	310
250	25	none	102	46	28.9	10.4	114
250	760	None	107	44	28.6	10.4	0

deep and ultra-deep X-ray lithography, as the irradiation proceeds, successive chemical modifications of the resist material occur, particularly at high fluence, where the energy-loss mechanism may become very complex owing to multiple overlap and where scission and recombination reactions may also generate heat.

Among the possible effects induced by irradiation, one can list:

(i) A gradient of dose deposition develops within the resist thickness, the absorption of the X-ray spectrum being non-uniform within the PMMA resist because of the non-linear behaviour of the polymer as illustrated in Fig. 7. This causes a non-uniformity of material modifications and properties within the resist, such as molecular mass distribution, and maybe even chemical structure and crystallinity, glass transition and melting temperatures, thermal conductivity, volume change, stress *etc.* In particular, the PMMA resist becomes more sensitive to temperature, because of the already irradiated part, as the irradiation proceeds, especially on top of the resist where most of the low-energy radiation is preferentially absorbed, decomposing the top of the resist before the bulk of the resist.

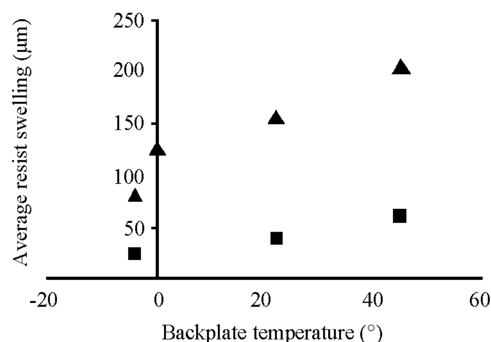

Figure 6
Swelling of acrylic sheet with variation in temperature of the sample backplate during exposure. The squares and triangles correspond to samples exposed while the storage ring was operated at 1.3 and 1.5 GeV electron energy, respectively. The exposure conditions were beamline XRLM3; 125 µm Be window; 300 µm × 40 mm × 40 mm PMMA resist; Goodfellow (CQ); pre-exposure annealing at 353 K for 1 h (ramped) in N_2; dose at resist bottom = 3 kJ cm^{-3}. Mask: large mesh; scan length: 2.5 cm; scan velocity: 6.25 mm s^{-1}; He pressure in chamber: 100 T. For accuracy of swelling measurements, see §2.

(ii) The presence and repartition of microvoids within the material modifies the permeation properties of the polymer matrix and the diffusion path of the evolved gases. This might also affect the dimensional accuracy of the pattern transfer.

(iii) The gas generation rate in thick PMMA samples may be larger than the diffusion rate, causing gas accumulation in the polymer layer, especially in the exposed area that has become porous. An excessive amount of gas build-up in the PMMA may occur, causing the swelling of the resist surface during or/and after exposure. In particular, this occurs when high-intensity beams are being used.

(iv) Swelling of the resist is strongly dependent on the X-ray exposure conditions as well as on the nature, treatment and thermal properties of the resist layer:

(*a*) The swelling amplitude is pattern dependent, as the total dose integrated on one field size is distributed depending on the ratio

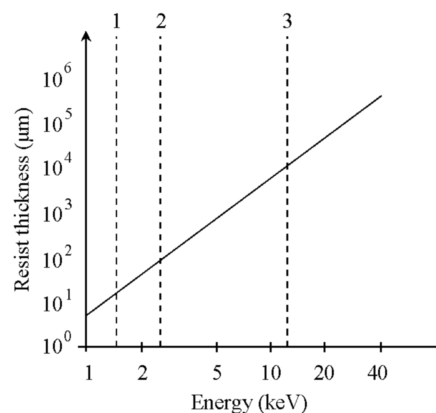

Figure 7
Absorption length of PMMA as a function of incident photon energy. In this graph (Khan Malek *et al.*, 1998) the absorption lengths as a function of monochromatic photon energies were calculated from mass attenuation coefficients tabulated for the photoelectric effect and Compton scattering (at higher energies) by the National Institute of Standards and Technology (NIST) (http://physics.nist.gov/PhysRefData/XrayMassCoef/). In reality, with the synchrotron radiation spectrum being broadband, a range of absorption depths exists within the resist. The critical energies (E_c) of CAMD photon spectra from bending magnets of the storage ring operated at 1.3 and 1.5 GeV electron energies are indicated by vertical lines 1 (E_c = 1.7 keV) and 2 (E_c = 2.6 keV), respectively, and from the wiggler superconducting magnets at 7.5 T by line 3 (E_c = 11.2 keV).

between transmitting and opaque parts of the mask. For this reason, we limited our study to the variation of amplitude corresponding to one pattern only.

(*b*) Swelling depends on the thickness of the resist as well as the source of the resist.

(*c*) A higher dose resulted in increased swelling. As thicker resists require higher incident dose, more swelling occurred with thicker resists.

(*d*) Uniformity in dose distribution across the depth of the resist, expressed by the top-to-bottom dose ratio, was also an important factor for the control of radiation-induced swelling. The use of higher energy corresponding to longer penetration depth and a better dose distribution within the resist height gave lower top-to-bottom dose ratios. The resist could then bear a higher dose and the damage threshold of the resist was higher.

(*e*) Higher deposition dose resulted in increased resist swelling. Swelling, however, was a function not only of the dose deposition and dose gradient within the resist bulk but also of the dose deposition rate, which depended on the incident power density on the resist.

(*f*) At fixed dose deposition, the swelling amplitude was reduced and the damage threshold was increased for a lower deposition rate, which favoured the lower photon power associated with lower electron energy or smaller electron current in the ring. At fixed deposition rate, a shorter scan length and higher scan speed minimized the swelling amplitude.

(*g*) Thermal treatment of the acrylic sheet before exposure reduced the amplitude of the swelling significantly during exposure. This effect is believed to be due to a (partial) elimination of residual MMA monomer content as demonstrated by gas chromatography–mass spectroscopy of the PMMA samples before and after annealing (Henry *et al.*, 1999). However, the annealed acrylic sheet was observed to swell slowly for up to several days after exposure. If we want to be sure that swelling does not affect the pattern accuracy, the 'recipe' is to develop the wafer immediately.

(*h*) The swelling amplitude was also found to be a function of the pressure differential existing between the atmosphere of the exposure chamber surrounding the resist sample and the built-up gas pressure below the resist surface, favouring exposure at higher ambient pressure.

(*i*) The swelling amplitude was also reduced by lowering the temperature of the sample during irradiation.

One of the major problems of commercialization of LIGA is cost and throughput (Guckel *et al.*, 1996; Saile, 1998). Using a higher current in the storage ring or working at a higher energy does increase the radiation power intensity of the incident beam. However, the benefit of such an approach is limited by the intrinsic properties, in particular absorptive and thermal, of the PMMA resist for withstanding a maximum dose and dose deposition rate. The maximum power that can be delivered to a given thickness is also limited by how this power is being delivered. To increase the throughput of the beamline while using PMMA, a high dose rate needs to be better distributed over the thickness of the resist so that each volume is exposed with a tolerable dose rate and power density. The use of higher-energy photons in ultra-deep X-ray lithography allows for a larger volume of resist to be exposed in the same amount of time owing to the increased penetration depth of the harder X-rays. Therefore, the dose rate deposited in a given volume can be reduced, especially at the top of the resist, minimizing the threshold for resist swelling and damage. This effect is exploited for thicker resist exposure or parallel exposure of multiple resist layers (Siddons *et al.*, 1994, 1998). At CAMD, when the new source of harder X-rays with a critical energy of 11.2 keV is operational on a routine basis, stacked exposures will be possible, which may lead to large-scale fabrication of high-aspect-ratio MEMS (Khan Malek *et al.*, 1998).

5. Conclusion

Swelling of the PMMA resist layer is due to the accumulation of gaseous by-products generated during the irradiation process. The amount of swelling depends on the total absorbed dose, the dose distribution and the rate of energy deposition inside the resist and is sensitive to parameters influencing those quantities.

Thin resist layers are well controlled.

Swelling for thick resist layers can be controlled by proper adjustment of various parameters during irradiation.

The synchrotron radiation spectrum needs to be accurately tailored to the thickness of the resist in order to ensure uniformity of absorbed dose distribution within the resist and reduction of resist swelling. This requirement is achieved using, when possible, proper ring energy and adequate filtering, and keeping the incident power density on the resist and dose deposition rate under a certain threshold.

The threshold for swelling is also a function of parameters affecting the dose deposition rate, such as the current in the ring, and of the uniformity of dose deposition, which is modified by the filtering conditions during exposure. This issue is particularly severe with very thick and ultra-thick resists and when high-intensity beams are being used.

The variation of other exposure conditions affects the swelling response: an increase in helium pressure in the exposure chamber and/or increase in scan velocity reduces swelling, whereas an increase in scan length causes enhanced swelling and an increase of the temperature of the sample.

Swelling also depends on the thickness, source and thermal treatment of the resist. Pre-exposure annealing of clinical-grade high-molecular-weight acrylic sheets was found to reduce swelling significantly during exposure, though not during post-exposure storage.

In order to ensure pattern accuracy, immediate development of the wafer after exposure is required.

Louis Rupp, CAMD, is thanked for his help in instrumentation on the X-ray microfabrication beamline, and Raghu Bonghu for his help in preparing samples. The State of Louisiana and the Space and Naval Warfare Systems Center (under the DARPA Grant N66001-98-1-8926) are acknowledged for salary support.

References

Becker, E. W., Ehrfeld, W., Hagmann, P., Maner, A. & Munchmeyer, D. (1986). *Microelectron. Eng.* **4**, 35–56.

Chaudhuri, B., Guckel, H., Klein, J. & Fischer, K. (1997). *Microsyst. Technol.* **4**, 159–162.

CXrL Toolset (1966). University of Wisconsin-Madison, USA.

De Carlo, F., Mancini, D. C., Lai, B. & Song, J. J. (1998). *Microsyst. Technol.* **4**, 86–88.

Garrett, R. W., Hill, J. T., Le, T. T., Milne, A., O'Donnell, J. H., Perera, S. M. C. & Pomery, P. J. (1991). *ACS Symposium Series* 475, *Radiation Effect on Polymers*, edited by J. A. Moore, J. O. Choi, R. L. Clough & S. W. Shalaby, pp. 146–155. New York: Oxford University Press.

Guckel, H. (1996). *Rev. Sci. Instrum.* **67**, 1–5.

Henry, A. C., McCarley, R. L., Das, S. & Khan Malek, C. G. (1999). *J. Electrochem. Soc.* **146**, 2631–2636.

Henry, A. C., McCarley, R. L., Das, S., Khan Malek, C. G. & Poche, D. S. (1998). *Microsyst. Technol.* **4**, 104–109.

Hiraoka, H. (1977). *IBM J. Res. Develop.* **21**, 121–130.
Ichikawa, T. & Yoshida, H. (1994). *J. Polym. Sci. A*, **32**, 2487–2492.
Khan Malek, C., Saile, V., Manohara, H. & Craft, B. (1998). *J. Synchrotron Rad.* **5**, 1095–1098.
Lehockey, E. M., Reid, I. & Hill, I. (1988). *J. Vac. Sci. Technol. A*, **6**, 2221–2225.
Moldovan, N. (1999). *Proc. SPIE*, **3875**, 155–163.
Moore J. A. & Choi, J. O. (1991). *ACS Symposium Series* 475, *Radiation Effect on Polymers*, edited by J. A. Moore, J. O. Choi, R. L. Clough & S. W. Shalaby, pp. 156–192. New York: Oxford University Press.
Moreau, W. M. (1988). *Semiconductor Lithography: Principles, Practices and Materials.* New York: Plenum.
Okudaira, K. K., Hasegawa, S., Sprunger, P. T., Morikawa, E. & Saile, V. (1998). *J. Appl. Phys.* **83**, 4292–4298.
Saile, V. (1998). *Strategies for LIGA Implementation*, edited by H. Reidl and E. Obermeier, pp. 25–30, Microsystem Technologies 98, Sixth International Conference on Micro, Opto, Mechanical Systems and Components. Potsdam, Germany: VDE-Verlag.
Schmalz, O., Hess, M. & Kosfeld, R. (1996). *Angew. Makromol. Chem.* **239**, 63–77, 79–91.
Siddons, D. P., Johnson, E. D. & Guckel, H. (1994). *Synchrotron Rad. News*, **7**, 16–18.
Siddons, D. P., Johnson, E. D. & Guckel, H. (1998). *Microsyst. Technol.* **4**, 70–73.
Tinone, M. C. K. & Tanaka, K. (1995). *J. Vac. Sci. Technol. A*, **13**, 1885–1892.
Waali, E. E., Scott, J. D., Vladimirsky, O., Vladimirsky, Y., Hayataka, K. M. & Klopf, J. M. (1998). *Proc. SPIE*, **3331**, 518–524.
Wollersheim, O. & Hormes, J. (1996). *Chem. Phys.* **204**, 129–134.
Wollersheim, O., Zumaque, H., Hormes, J., Kadereit, D., Langen, J., Haussling, L., Hoessel, P. & Hoffmann, G. (1995). *Nucl. Instrum. Methods Phys. Res. B*, **97**, 273–278.
Yates, B. W. & Shinozaki, D. M. (1993). *J. Polym. Sci. B*, **31**, 1779–1784.

Received 14 March 2001 • Accepted 21 February 2003